



---

<sup>b</sup>  
**UNIVERSITÄT  
BERN**

# **3D Metric Fields**

## **A Novel Approach to a New Idea**

### **Bachelor Thesis**

Florin Achermann  
from  
Bern, Switzerland

Faculty of Science, University of Bern

15. September 2023

Prof. David Bommes  
Computer Graphics Group  
Institute of Computer Science  
University of Bern, Switzerland



# Abstract

Lorem ipsum dolor sit amet, consectetur adipiscing elit, sed do eiusmod tempor incididunt ut labore et dolore magna aliqua. Ut enim ad minim veniam, quis nostrud exercitation ullamco laboris nisi ut aliquip ex ea commodo consequat. Duis aute irure dolor in reprehenderit in voluptate velit esse cillum dolore eu fugiat nulla pariatur. Excepteur sint occaecat cupidatat non proident, sunt in culpa qui officia deserunt mollit anim id est laborum.



# Contents

<b>1</b>	<b>Introduction</b>	<b>1</b>
<b>2</b>	<b>Mathematical Background</b>	<b>3</b>
2.1	Differential Geometry . . . . .	3
2.1.1	Manifold . . . . .	3
2.1.2	Tangent space, Tangent bundle . . . . .	3
2.1.3	Cotangent space, Cotangent bundle . . . . .	3
2.1.4	Tensors . . . . .	4
2.1.5	Differential Forms, Exterior Derivative . . . . .	4
2.1.6	Riemannian metric, $g$ -orthonormality . . . . .	4
2.1.7	Connection, Covariant derivative, Parallel transport . . . . .	4
2.2	Frame fields . . . . .	5
2.2.1	Integer-grid maps . . . . .	5
2.2.2	Frame fields as a relaxation . . . . .	6
<b>3</b>	<b>Connection One-Form <math>\omega</math></b>	<b>9</b>
3.1	Smoothness measure . . . . .	10
3.2	Connection evaluation . . . . .	10
<b>4</b>	<b>Calculation of rotation coefficient</b>	<b>13</b>
4.1	Piecewise linear discretization . . . . .	13
4.2	Recursive subdivision . . . . .	14
<b>5</b>	<b>Algorithm for <math>R</math> between two arbitrary points in a mesh</b>	<b>17</b>
5.1	Framework . . . . .	17
5.1.1	A note on orientation tests . . . . .	18
5.2	Algorithm <i>tetFinder</i> . . . . .	19
<b>6</b>	<b>Frame Field optimization</b>	<b>21</b>
<b>7</b>	<b>Experiments</b>	<b>23</b>
<b>8</b>	<b>Conclusion</b>	<b>25</b>
<b>A</b>	<b>Extra material</b>	<b>27</b>



# Chapter 1

## Introduction

In many applications of computer graphics or engineering, the geometry of objects has to be described in some way. Finite elements encode various information such as physical properties to be used in e.g. stress simulations. While it is possible for simple objects such as spheres or planes to describe them with analytical formulas, this is unfeasible for arbitrary objects of any shape. To describe any geometric object, it is discretized and encoded as a mesh. Volumetric meshes are used to encode the surface and the interior of an object. The most common types of volumetric meshes are tetrahedral and hexahedral meshes. Hexahedral meshes, that is a decomposition into cube-like elements, are usually preferred due to their superior numerical accuracy and faster compute time. However, automatically generating high-quality meshes remains a hard challenge in computer graphics. A promising research direction is through the use of frame fields [12].

A *frame field* can be seen as a generalization of vector fields. They prescribe a *frame* to each point on an object, that is, three linearly-independent vectors. Each frame locally represents the orientation and deformation of a cube. Consequently, frame fields must be so called boundary-aligned: At the boundary of an object, one vector of the frame must be aligned with the surface normal as hexahedral elements (*short: hex element*) should align at the boundary. Then, the objective is to find the “best” frame field. Usually, “best” is measured in the smoothness of the frame field. Smoothness is measured with the Dirichlet energy  $\int_{\Omega} \|\nabla \phi\|^2 dx$ , where  $\phi$  is a frame, and we measure how much these frames twist and rotate within the object.

To allow for non-uniform and anisotropic hex elements, we introduce *metric fields*. Optimizing the frame field in this new metric (instead of the usual euclidean metric) then results in elements that are uniform and isotropic in this new metric. To this end, the expression for the Dirichlet energy must be changed. We will show how to calculate a special rotation matrix  $R$ , which describes how frames are aligned in the new metric.

In this thesis, we rederive how to pull back the metric with the rotation coefficient  $R$  such that we can measure the Dirichlet energy in the usual cartesian coordinates as described in *Metric-Driven 3D Frame Field Generation*[4]. The necessary mathematical background is introduced in Section 2. In Section 3, by focusing on integrability of the frame field, we derive the connection  $\omega$  under our new metric field and how to evaluate it. Section 4 discusses how the metric field is piecewise-linearly discretized as a tetrahedral mesh and how the rotation coefficient  $R$  to align frames in the metric is calculated within a specific tetrahedron. Because in general,  $R$  is needed between arbitrary points in the metric field, a robust tetrahedron finder algorithm is presented in Section 5. We briefly explain how the actual frame field optimization works in Section ?? . The whole frame field generation is tested with some experiments in Section 7. We conclude in Section 8.





## Chapter 2

# Mathematical Background

A solid mathematical introduction is key to understanding how and why the approach in this thesis work. This chapter serves as a primer to differential geometry and frame fields.

### 2.1 Differential Geometry

We will make heavy use of differential geometry in chapter chapter 3. I introduce the basic concepts what we will use, but I refrain from giving any proofs. I will give definitions only as far as we need it. These definitions will by no means be exhaustive. The following is an incomplete summary of concepts that we need presented in *Introduction to smooth manifolds*[?].

#### 2.1.1 Manifold

A manifold  $\mathcal{M}$  is a space that locally looks like Euclidean space. More exactly, a  $n$ -manifold is a topological space, where each point on the manifold has an open neighborhood that is locally homeomorphic to an open subset of Euclidean space  $\mathbb{R}^n$ . A manifold can be equipped with additional structure. For example, we can work on *smooth manifolds*. In simple terms, a manifold is *smooth* if it is similar enough to  $\mathbb{R}^n$  that we can do Calculus like differentiation or integration on it. For this, each point on the manifold must be locally *diffeomorphic* to an open subset of  $\mathbb{R}^n$  space.

#### 2.1.2 Tangent space, Tangent bundle

There are many equivalent definitions for the tangent space. One definition is for each point  $p$  in the manifold  $\mathcal{M}$ , the tangent space  $T_p\mathcal{M}$  consists of  $\gamma'(0)$  for all differentiable paths  $\gamma : (-\varepsilon, \varepsilon) \rightarrow \mathcal{M}$  with  $p = \gamma(0)$ . The tangent space is a vector space which has the same dimension as its manifold, which is 3 in our case. These tangent spaces can be “glued” together to form the *tangent bundle*  $T\mathcal{M} = \sqcup_{p \in \mathcal{M}} T_p\mathcal{M}$ , which itself is a manifold of dimension  $2n$ . An element of  $T\mathcal{M}$  can be written as  $(p, v)$  with  $p \in \mathcal{M}$  and  $v \in T_p\mathcal{M}$ . This admits a natural projection  $\pi : T\mathcal{M} \rightarrow \mathcal{M}$ , which sends each vector  $v \in T_p\mathcal{M}$  to the point  $p$  where it is tangent:  $\pi(p, v) = p$ . A *section*  $\sigma : \mathcal{M} \rightarrow T\mathcal{M}$  is a continuous map, with  $\pi \circ \sigma = \text{Id}_{\mathcal{M}}$ . Sections of  $T\mathcal{M}$  are tangent vector fields on  $\mathcal{M}$ .

#### 2.1.3 Cotangent space, Cotangent bundle

The dual space  $V^*$  of a vector space  $V$  consists of all linear maps  $\omega : V \rightarrow \mathbb{R}$ . We call these functionals *covectors* on  $V$ .  $V^*$  is itself a vector space, with the same dimension as  $V$  and operations like addition and scalar multiplication can be performed on its elements. Any element in a vector space can be expressed as a finite linear combination of its basis. This basis is called the *dual basis*. Thus, we call the dual space of the vector space  $T_p\mathcal{M}$  its *cotangent space*, denoted by  $T_p^*\mathcal{M}$ . As before, the disjoint union of  $T_p^*\mathcal{M}$  forms the *cotangent bundle*:  $T^*\mathcal{M} = \sqcup_{p \in \mathcal{M}} T_p^*\mathcal{M}$ . Defined analogously from above, sections  $\sigma$  on  $T^*\mathcal{M}$  define *covector fields* or *1-forms*.

### 2.1.4 Tensors

Before we can introduce differential forms in the next paragraph, we need to go a little bit into *tensors*. In simple words, tensors are real-valued, multilinear functions. A map  $F : V_1 \times \dots \times V_k \rightarrow W$  is multilinear, if  $F$  is linear in each component. For example, the dot product in  $\mathbb{R}^n$  is a tensor. It takes two vectors and is linear in each component - bilinear. Another example is the *Tensor Product of Covectors*: Let  $V$  be a vector space and take two covectors  $\omega, \eta \in V^*$ . Define the new function  $\omega \otimes \eta : V \times V \rightarrow \mathbb{R}$  by  $\omega \otimes \eta(v_1, v_2) = \omega(v_1)\eta(v_2)$ . It is multilinear, because  $\omega$  and  $\eta$  are linear. We look at a special class of tensors, the *alternating tensors*. A tensor is alternating, if it changes sign whenever two arguments are interchanged, i.e.  $\omega(v_1, v_2) = -\omega(v_2, v_1)$ . A covariant tensor field over a manifold defines a covariant tensor at each point on the manifold, covariant because the tensor is over the cotangent space  $T_p^*\mathcal{M}$ . An alternating tensor field is called a *differential form*.

### 2.1.5 Differential Forms, Exterior Derivative

Recall that a section from  $T^*\mathcal{M}$  is called a differential 1-form, or just 1-form. Define the *wedge product* (or *exterior product*) between two 1-forms:

$$(\omega \wedge \eta)_p = \omega_p \wedge \eta_p$$

Notice the similarity to the *Tensor Product of Covectors*: We get a new map, (a 2-form):

$$\omega \wedge \eta : T\mathcal{M} \times T\mathcal{M} \rightarrow \mathbb{R}$$

The wedge product is antisymmetric, therefore  $\omega \wedge \eta = -\eta \wedge \omega$  for 1-forms  $\omega$  and  $\eta$ . We denote by  $\Omega^k(\mathcal{M})$  the space of differential  $k$ -forms on  $\mathcal{M}$ . There is a natural differential operator  $d$  on differential forms we call *exterior derivative*. It maps  $k$ -forms to  $(k+1)$ -forms, i.e.  $d : \Omega^k(\mathcal{M}) \rightarrow \Omega^{k+1}(\mathcal{M})$  and has the the following properties:

- $df$  is the ordinary differential of a smooth function  $f$ . Smooth functions are 0-forms.
- $d(d\alpha) = 0$
- $d(\alpha \wedge \beta) = (d\alpha \wedge \beta) + (-1)^k(\alpha \wedge d\beta)$  for a  $k$ -form  $\alpha$ . (Leibnitz Rule)

In section 3 we will need what  $d\omega$  is for some smooth 1-form  $\omega$ , the calculation will be done there. For now, just note that any arbitrary smooth 1-form can be written as  $\omega = Fdx + Gdy + Hdz$  for some appropriate smooth functions  $F, G, H$ .

### 2.1.6 Riemannian metric, $g$ -orthonormality

Inner products are examples of symmetric tensors. They allow us to define lengths and angles between vectors. We can apply this idea to manifolds. A Riemannian metric  $g$  is a symmetric positive-definite tensor field at each point. If  $\mathcal{M}$  is a manifold, the pair  $(\mathcal{M}, g)$  is called a *Riemannian manifold*. Let  $g$  be the Riemannian metric on  $\mathcal{M}$  and  $p \in \mathcal{M}$ , then  $g_p$  is an inner product on  $T_p\mathcal{M}$ . We write  $\langle \cdot, \cdot \rangle_g$  to denote this inner product. Any Riemannian metric can be written as positive-definite symmetric matrix, which allows for this simple form:  $\langle v, w \rangle_g = v^\top gw$ .

Such a new metric allows for the definition of  *$g$ -orthonormality*: A basis  $[e_1, e_2, e_3]$  of  $T_p\mathcal{M}$  is  *$g$ -orthonormal* if  $\langle e_i, e_j \rangle_g = \delta_{ij}$ .

### 2.1.7 Connection, Covariant derivative, Parallel transport

A connection defines how two different tangent spaces are connected to each other, such that tangent vector fields can be differentiated. There is an infinite amount of connections on a manifold. An *affine connection*  $\nabla$  is a bilinear map that takes two tangent vector fields  $X, Y$  and maps it to a new tangent vector field  $\nabla_X Y$  on  $\mathcal{M}$  such that

- $\nabla_{fX}Y = f\nabla_XY$ , where  $f \in C^\infty(\mathcal{M}, \mathbb{R})$
- $\nabla_X(fY) = f\nabla_XY + (Xf)Y$  for  $f \in C^\infty(\mathcal{M}, \mathbb{R})$ , it satisfies the Leibnitz rule in the second variable

We call  $\nabla_XY$  the *covariant derivative of  $Y$  in the direction of  $X$* . A connection  $\nabla$  defines the parallel transport of a vector along a curve. Given a curve  $\gamma : [0, 1] \rightarrow \mathcal{M}$  and a vector  $v_0 \in T_{\gamma(0)}\mathcal{M}$ , there exists a unique parallel vector field  $V : [0, 1] \rightarrow T\mathcal{M}$  along  $\gamma$  such that  $V(0) = v_0$  [6]. Recall: a vector field  $V$  along  $\gamma$  means  $\pi(V(t)) = \gamma(t)$ . The uniqueness and existence is a consequence of the vector field  $V$  being the solution of  $\nabla_{\dot{\gamma}(t)}V(t) = 0$  defining a linear ordinary differential equation with initial condition  $V(0) = v_0$ . This vector field  $V(t)$  is called the *parallel transport* of  $v_0$  along  $\gamma$ . It is “parallel” in the sense that the transported vector does not change within the tangent space. See figure 2.1 for an illustration in 2D.

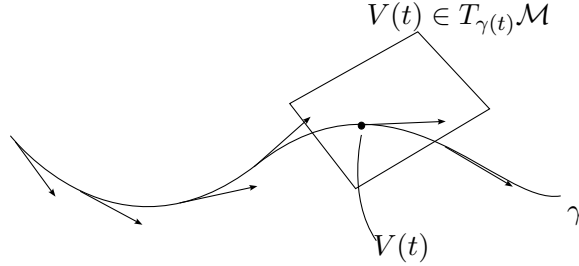


**Figure 2.1.** A parallel vector field  $V(t)$  along a curve  $\gamma$ . Each  $V(t) \in T_{\gamma(t)}\mathcal{M}$  and  $\nabla_{\dot{\gamma}(t)}V(t) = 0$ , so each vector that is drawn is parallel to each other.

## 2.2 Frame fields

Recall from the introduction that we are trying to find a hexahedral mesh for some geometric object. In the following sections, the key idea to tackle this problem through *integer-grid maps* is discussed and how the problem is relaxed through *frame fields*.

### 2.2.1 Integer-grid maps

In 2D, integer-grid maps have proven to be reliable in generating the analogue of hexahedral meshes, quad meshes [2]. The goal is to use the same approach, but in three dimensions. The objective is to find a parametrization  $\phi : \mathcal{M} \rightarrow \mathbb{R}^3$ , which embeds the 3-dimensional object to be meshed onto a 3-dimensional voxel grid, where the inverse  $\phi^{-1}$  maps the deformed grid back onto the object to recover a shape-aligned hexahedral mesh, see figure 2.2 for an illustration. This is called an integer-

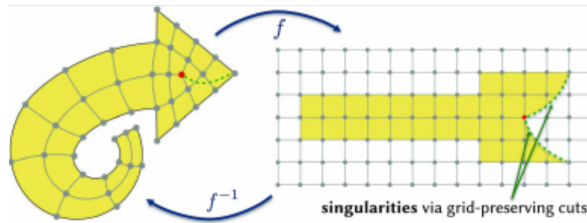


**Figure 2.2.** Idea of quadrangulation with integer-grid maps in 2D

grid map and by minimizing distortion and satisfying boundary alignment, a hexahedral mesh could be extracted. However, this is a hard mixed-integer and non-convex optimization problem for which no current optimization technique is available that would result in an acceptable solution.

### 2.2.2 Frame fields as a relaxation

By taking the Jacobian of the parametrization,  $\nabla\phi$ , we get a mapping  $\nabla\phi : \mathcal{M} \rightarrow \mathbb{R}^{3 \times 3}$  of *frames*, a *frame field*. The idea of frame fields is then to search for an approximation of  $\nabla\phi$ . If  $F : \mathcal{M} \rightarrow \mathbb{R}^{3 \times 3}$  is the approximation of  $\nabla\phi$ , we can solve for  $\phi : \mathcal{M} \rightarrow \mathbb{R}^3$  with

$$\min_{\phi} \int_{\mathcal{M}} \|\nabla\phi F - \text{Id}\|^2$$

where  $\|\cdot\|$  is the Frobenius norm. If this is sufficiently small, then  $F^{-1} \approx \nabla\phi$  and the extracted hexahedral mesh closely follow the integer-grid isolines. A frame locally represents the edges of a deformed cube. We can think of a frame field as the composition of three vector fields and as a relaxation of the original problem. However, frame fields can contain singularities that the underlying vector fields do not contain [9] and contain types of singularities that cannot appear in hex meshes [8]. These singularities are said to be non-meshable. The problem of non-meshability is not discussed further here, but it is something to be aware of.

We treat a frame  $F$  as a set of 3 linearly independent vectors  $\{F_1, F_2, F_3\}$  which we can collect into a matrix  $F = (F_1, F_2, F_3) \in \mathbb{R}^{3 \times 3}$ . Notice that many of these frames are equivalent. There are  $2^3$  choices of the sign, and  $3!$  possible permutations, which gives  $2^3 \cdot 3! = 48$  equivalent frames. Since we want non-degenerate frames and the same orientation through the grid, the constraint  $\det(F) > 0$  is imposed, which leaves 24 equivalent frames. Equivalence of frames is then defined as

$$F_u \sim F_v \iff \exists R \in \mathcal{O} : F_u = RF_v$$

where  $\mathcal{O}$  is the *chiral cubical symmetry group* [9]. These symmetries make the optimization for frame fields more complicated. To handle these symmetries, we use the spherical harmonics based representation [5]. The idea is to use the polynomial  $x^4 + y^4 + z^4$  to express the frames as rotations. Under the restriction of the polynomial to the sphere, that is  $\mathbb{S}^2 \rightarrow \mathbb{R}$ , the octahedral frames are invariant under the chiral cubical symmetry group. However, the spherical harmonics manifold is 9-dimensional, so not all vectors in the spherical harmonics represent valid frames, since rotations only exhibit 3 degrees of freedom. While optimizing the frame field, some kind of “average” of two frames will be done. This averaging makes sense in the spherical harmonics space, but the result may be outside the valid space of frames. A projection from the spherical harmonics space back to the valid space of frames will be needed, see fig. 2.3 [13].

When a frame  $F$  has orthonormal columns, the resulting hex elements look like unit cubes. By introducing a metric  $g$ , we can control the size and shear of the cubes by relaxing the orthonormality constraint to  $g$ -orthonormality when

$$F^{-1}gF = \text{Id}$$

holds. We can decompose the frame field  $F$  into a rotational part  $R : \mathcal{M} \rightarrow \text{SO}(3)$  and a symmetric metric part  $g^{-1/2}$  (akin to the polar decomposition of linear transformations) [10], that is  $F = g^{-1/2}R$ , see figure 2.4.

TODO: Frame field goals

- Dirichlet energy, what are we optimizing
- Requirements for the frame field -  $\zeta$  integrability + boundary alignment

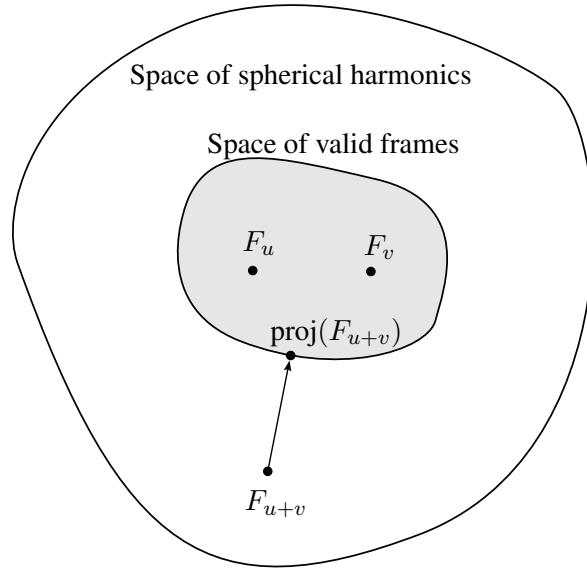


**Figure 2.3.** Combination of two valid frames leads to a resulting frame outside the valid frames. A projection to the nearest valid frame is done.

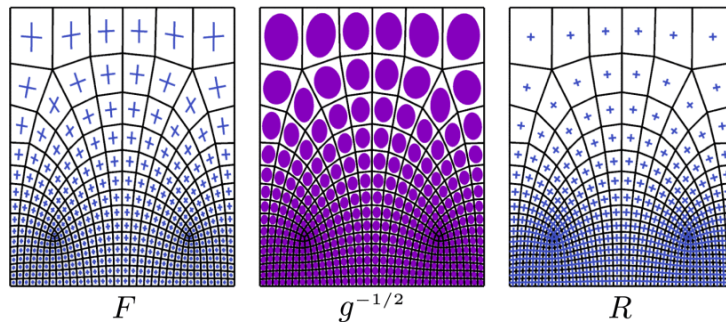


**Figure 2.4.** Factorization of a  $g$ -orthogonal frame field into a symmetric metric part  $g^{-1/2}$  and a rotational part  $R$  (Figure from [4]).



## Chapter 3

# Connection One-Form $\omega$

TODO: introduction, why are we doing this

A vector field  $U$  is integrable, if and only if  $\nabla \times U = 0$ , which means the vector field has vanishing curl everywhere. We can express this more naturally with the language of differential forms: The curl can be written as the exterior derivative  $d$  of a one-form  $\alpha$ . A one-form (more generally, a differential form) is closed, if  $d\alpha = 0$ . Therefore, the local integrability can be expressed as the closedness of a one-form. We want  $F^{-1}$  (TODO: why  $F^{-1}$ ) to be integrable. To achieve local integrability for, it suffices to make  $R$  locally integrable. We can think of a rotation field  $R$  as the composition of 3 vector fields

$$R = \begin{bmatrix} | & | & | \\ R_1 & R_2 & R_3 \\ | & | & | \end{bmatrix}$$

where  $R_i : \mathbb{R}^3 \rightarrow \mathbb{R}^3$  is a vector field. We can therefore construct a vector-valued one-form, given  $p = (x, y, z)^\top$  in Euclidean coordinates

$$\alpha \triangleq F^{-1}dp = R^\top g^{1/2}dp$$

where  $dp = (dx, dy, dz)^\top$  is the common orthonormal one-form basis.

$$R \text{ locally integrable} \iff \mathbf{0} = d\alpha$$

Some reformulations yield:

$$\begin{aligned} \mathbf{0} = d\alpha &= d(R^\top g^{1/2}dp) \stackrel{(1)}{=} dR^\top \wedge (g^{1/2}dp) + R^\top d(g^{1/2}dp) \\ &= R^\top (\omega \wedge (g^{1/2}dp) + d(g^{1/2}dp)) \end{aligned}$$

where for (1), the Leibnitz Rule for the exterior derivative is applied, and we define

$$\omega = RdR^\top \in \mathfrak{so}(3).$$

**Remark.**  $\omega$  is an antisymmetric matrix-valued one-form (every element is a one-form).

*Proof.* We differentiate the orthogonality condition of the rotation matrix  $R$  (taking the derivative w.r.t. every element):

$$\begin{aligned} Id &= RR^\top \\ d(Id) &= d(RR^\top) \\ \mathbf{0} &= dRR^\top + RdR^\top \\ \mathbf{0} &= (RdR^\top)^\top + RdR^\top \\ -(RdR^\top)^\top &= RdR^\top \end{aligned}$$

□

Elements of the Lie algebra  $\mathfrak{so}(3)$  can be thought as infinitesimal rotations and  $\omega$  can be used as a connection one-form. The Lie algebra  $\mathfrak{so}(3)$  has manifold structure, but for our purposes, it suffices to know that elements are antisymmetric matrices. To make  $R$  locally integrable, we find  $\omega$  such that the one-form  $\alpha$  is closed ( $d\alpha = 0$ , curl-free), then try to match the  $\omega$  with  $R$ , which can be expressed as

$$\min_{R \in SO(3)} \|RdR^T - \omega\|^2.$$

### 3.1 Smoothness measure

### 3.2 Connection evaluation

To find  $\omega$ , we use the above equation

$$\mathbf{0} = R^\top (\omega \wedge (g^{1/2} dp) + d(g^{1/2} dp)) \iff \mathbf{0} = \omega \wedge (g^{1/2} dp) + d(g^{1/2} dp)$$

and reformulate into a linear system. We represent the antisymmetric matrix-valued one-form  $\omega$

$$\omega = \begin{bmatrix} 0 & \omega_{12} & -\omega_{31} \\ -\omega_{12} & 0 & \omega_{23} \\ \omega_{31} & -\omega_{23} & 0 \end{bmatrix}$$

by  $\begin{bmatrix} \omega_{23} & \omega_{31} & \omega_{12} \end{bmatrix} = \begin{bmatrix} dx & dy & dz \end{bmatrix} W$ . We write  $W = [W_1, W_2, W_3]$ ,  $W_i \in \mathbb{R}^3$ . That is,  $W$  is the matrix with the coefficients for the one-forms, e.g.  $W_1 = [(\omega^{23})_1, (\omega^{23})_2, (\omega^{23})_3]^\top$ . Recall, a one-form can be expressed as

$$\omega_{ij} = (\omega^{ij})_1 dx + (\omega^{ij})_2 dy + (\omega^{ij})_3 dz$$

So e.g.

$$\omega_{23} = \begin{bmatrix} dx & dy & dz \end{bmatrix} W_1 = (\omega^{23})_1 dx + (\omega^{23})_2 dy + (\omega^{23})_3 dz$$

We also write  $A = g^{1/2} = [A^1, A^2, A^3]$ . We use the equation  $\mathbf{0} = \omega \wedge (g^{1/2} dp) + d(g^{1/2} dp)$ . Let us start with the first part:

$$\begin{aligned} \omega \wedge g^{1/2} dp &= \begin{bmatrix} 0 & \omega_{12} & -\omega_{31} \\ -\omega_{12} & 0 & \omega_{23} \\ \omega_{31} & -\omega_{23} & 0 \end{bmatrix} \wedge \begin{bmatrix} A_1^1 & A_1^2 & A_1^3 \\ A_2^1 & A_2^2 & A_2^3 \\ A_3^1 & A_3^2 & A_3^3 \end{bmatrix} \begin{bmatrix} dx \\ dy \\ dz \end{bmatrix} \\ &= \begin{bmatrix} +\omega_{12} \wedge (A_2^1 dx + A_2^2 dy + A_2^3 dz) - \omega_{31} \wedge (A_3^1 dx + A_3^2 dy + A_3^3 dz) \\ -\omega_{12} \wedge (A_1^1 dx + A_1^2 dy + A_1^3 dz) + \omega_{23} \wedge (A_3^1 dx + A_3^2 dy + A_3^3 dz) \\ +\omega_{31} \wedge (A_1^1 dx + A_1^2 dy + A_1^3 dz) - \omega_{23} \wedge (A_2^1 dx + A_2^2 dy + A_2^3 dz) \end{bmatrix} \end{aligned}$$

It will get really messy if we calculate each component here, so let us calculate one component separately first:

$$\begin{aligned} \omega_{ij} \wedge (A_k^1 dx + A_k^2 dy + A_k^3 dz) &= ((\omega^{ij})_1 dx + (\omega^{ij})_2 dy + (\omega^{ij})_3 dz) \wedge (A_k^1 dx + A_k^2 dy + A_k^3 dz) \\ &= (\omega^{ij})_1 A_k^2 dx \wedge dy + (\omega^{ij})_1 A_k^3 dx \wedge dz \\ &\quad + (\omega^{ij})_2 A_k^1 dy \wedge dx + (\omega^{ij})_2 A_k^3 dy \wedge dz \\ &\quad + (\omega^{ij})_3 A_k^1 dz \wedge dx + (\omega^{ij})_3 A_k^2 dz \wedge dy \\ &= ((\omega^{ij})_1 A_k^2 - (\omega^{ij})_2 A_k^1) dx \wedge dy \\ &\quad + ((\omega^{ij})_2 A_k^3 - (\omega^{ij})_3 A_k^2) dy \wedge dz \\ &\quad + ((\omega^{ij})_3 A_k^1 - (\omega^{ij})_1 A_k^3) dz \wedge dx \end{aligned}$$



where we use the fact that  $dx \wedge dx = 0$  and  $dx \wedge dy = -dy \wedge dx$ . We can clean up the above expression using the cross product:

$$\begin{bmatrix} ((\omega^{ij})_2 A_k^3 - (\omega^{ij})_3 A_k^2) \\ ((\omega^{ij})_3 A_k^1 - (\omega^{ij})_1 A_k^3) \\ ((\omega^{ij})_1 A_k^2 - (\omega^{ij})_2 A_k^1) \end{bmatrix}^\top \begin{bmatrix} dy \wedge dz \\ dz \wedge dx \\ dx \wedge dy \end{bmatrix} = [W_i \times A^k]^\top \begin{bmatrix} dy \wedge dz \\ dz \wedge dx \\ dx \wedge dy \end{bmatrix}$$

We use the fact that  $[A_1, A_2, A_3] = [A^1, A^2, A^3]$  because  $A$  is symmetric, and  $W_1$  corresponds to  $\omega_{23}$ ,  $W_2$  to  $\omega_{31}$  and  $W_3$  to  $\omega_{12}$ . Second part:

$$d(g^{1/2} dp) = d(Adp) = d \left( \begin{bmatrix} A_1^1 & A_1^2 & A_1^3 \\ A_2^1 & A_2^2 & A_2^3 \\ A_3^1 & A_3^2 & A_3^3 \end{bmatrix} \begin{bmatrix} dx \\ dy \\ dz \end{bmatrix} \right)$$

Again, we can do this separately for each row:

$$\begin{aligned} & d(A_k^1 dx + A_k^2 dy + A_k^3 dz) \\ &= dA_k^1 \wedge dx + dA_k^2 \wedge dy + dA_k^3 \wedge dz \\ &= \frac{\partial A_k^1}{\partial x} dx \wedge dx + \frac{\partial A_k^1}{\partial y} dy \wedge dx + \frac{\partial A_k^1}{\partial z} dz \wedge dx \\ &+ \frac{\partial A_k^2}{\partial x} dx \wedge dy + \frac{\partial A_k^2}{\partial y} dy \wedge dy + \frac{\partial A_k^2}{\partial z} dz \wedge dy \\ &+ \frac{\partial A_k^3}{\partial x} dx \wedge dz + \frac{\partial A_k^3}{\partial y} dy \wedge dz + \frac{\partial A_k^3}{\partial z} dz \wedge dz \\ &= \left( \frac{\partial A_k^3}{\partial y} - \frac{\partial A_k^2}{\partial z} \right) dy \wedge dz + \left( \frac{\partial A_k^1}{\partial z} - \frac{\partial A_k^3}{\partial x} \right) dz \wedge dx + \left( \frac{\partial A_k^2}{\partial x} - \frac{\partial A_k^1}{\partial y} \right) dx \wedge dy \\ &= (\nabla \times A_k)^\top \begin{bmatrix} dy \wedge dz \\ dz \wedge dx \\ dx \wedge dy \end{bmatrix} \end{aligned}$$

Finally, we can put everything together:

$$\begin{aligned} \mathbf{0} &= \begin{bmatrix} (W_3 \times A^2 - W_2 \times A^3 + \nabla \times A^1)^\top \\ (W_1 \times A^3 - W_3 \times A^1 + \nabla \times A^2)^\top \\ (W_2 \times A^1 - W_1 \times A^2 + \nabla \times A^3)^\top \end{bmatrix} \begin{bmatrix} dy \wedge dz \\ dz \wedge dx \\ dx \wedge dy \end{bmatrix} \\ &\iff \begin{bmatrix} (W_2 \times A^3 - W_3 \times A^2)^\top \\ (W_3 \times A^1 - W_1 \times A^3)^\top \\ (W_1 \times A^2 - W_2 \times A^1)^\top \end{bmatrix} \begin{bmatrix} dy \wedge dz \\ dz \wedge dx \\ dx \wedge dy \end{bmatrix} = \begin{bmatrix} (\nabla \times A^1)^\top \\ (\nabla \times A^2)^\top \\ (\nabla \times A^3)^\top \end{bmatrix} \begin{bmatrix} dy \wedge dz \\ dz \wedge dx \\ dx \wedge dy \end{bmatrix} \end{aligned}$$

Take the curl to the other side and switch order on the left-hand side to cancel the  $-1$ . As we are only interested in the 9 components of  $W$ , we omit the two-form basis and transform into a 9x9 linear system for  $W$ . We define  $A_\times$  and  $\text{vec}(\cdot)$  as

$$A_\times = \begin{bmatrix} 0 & -A_\times^3 & A_\times^2 \\ A_\times^3 & 0 & -A_\times^1 \\ -A_\times^2 & A_\times^1 & 0 \end{bmatrix}, \text{vec}(W) = \begin{bmatrix} W_1 \\ W_2 \\ W_3 \end{bmatrix}$$

with  $A_\times^i$  defined as

$$A_\times^i = [A_1^i \quad A_2^i \quad A_3^i]_\times = \begin{bmatrix} 0 & -A_3^i & A_2^i \\ A_3^i & 0 & -A_1^i \\ -A_2^i & A_1^i & 0 \end{bmatrix}$$

and  $\text{vec}(\cdot)$  turns a  $3 \times 3$ -matrix into a  $9 \times 1$ -vector by stacking the columns. With these two definitions, we can transform the above equality into a linear system

$$A_{\times} \text{vec}(W) = \text{vec}(\nabla \times A)$$

where  $\nabla \times A$  is just the curl applied to each column. This transformation can be checked by laboriously plugging in the definitions and comparing the coefficients. With tedious calculations, one can show that  $\det(A_{\times}) = -2 \det(A)^3 = -2 \det(g)^{3/2} < 0$ , which means this is a linear system that is solvable and can be used to calculate  $W$  at a point.

## Chapter 4

# Calculation of rotation coefficient

Recall that we want to measure the smoothness of the frame field by the Dirichlet energy.

We are interested in the rotation. Let  $p, q$  be points on the manifold and  $\ell$  a path connecting them. Let  $R : \mathcal{M} \rightarrow SO(3)$  be a rotation field, i.e.  $R(p), R(q)$  are orthogonal frames. Under the initial condition that  $R(p) = \text{Id}$ , the equation

$$R(q) = \exp(R_{pq}(\omega))R(p)$$

is a differential equation that corresponds to the parallel transport under the connection  $\omega$  of the frame along  $\ell$ . To recover this rotation  $R_{pq}$ , we integrate  $\omega$  along  $\ell$ .

**Setup** We parametrize the path by  $\ell(0) = a, \ell(1) = b$ . We resort to numerical integration for  $R_{ab}$  and cut the path into  $n$  small segments, i.e.

$$R_{ab} = R_n R_{n-1} \cdots R_1$$

where  $R_i = \exp(-\omega(\dot{\ell}(i\gamma))\gamma) = \exp((\int W^\top dp)_\times)$ , and  $\gamma$  is the length of a segment and  $\dot{\ell}(s) = \frac{\partial \ell}{\partial s}(s)$ . Calculating the exponential map of an antisymmetric matrix (which  $\omega \in \mathfrak{so}(3)$  is) can be done with Rodrigues' formula:

$$\exp(u_\times) = \text{Id} + \sin(\theta)\hat{u}_\times + (1 - \cos(\theta))\hat{u}_\times^2$$

where  $\theta = \|u\|_2$  is the rotation angle and  $\hat{u} = u/\theta$  is the rotation axis. We use the trapezoidal rule to evaluate the a short interval of the integral of  $W$ , which is given by

$$R_{ab} = \exp\left(\left(\frac{1}{2}(W_a + W_b)^\top(b - a)\right)_\times\right)$$

where  $W_a, W_b$  is solved for by the 9x9 linear system given by  $A_\times$  and  $\nabla \times A$ .

### 4.1 Piecewise linear discretization

We discretize our metric field with a tetrahedral mesh  $\mathcal{T}$ . At each vertex, we attach a metric and linearly interpolate with barycentric coordinates within a tet.

Let  $A_i \in \mathbb{R}^{3 \times 3}, i \in \{1, 2, 3, 4\}$  be the square root metrics at the vertices  $v_i \in \mathbb{R}^3$  of a tet, such that  $A_i^2 = g(v_i)$ . We represent a tet given by its four vertices by a 3x4 matrix, i.e.

$$\begin{pmatrix} | & | & | & | \\ v_1 & v_2 & v_3 & v_4 \\ | & | & | & | \end{pmatrix} \in \mathbb{R}^{3 \times 4}.$$

Any point  $p$  within the tet can then be represented as

$$p = \alpha v_1 + \beta v_2 + \gamma v_3 + \delta v_4$$

with  $\alpha, \beta, \gamma, \delta \geq 0$  and  $\alpha + \beta + \gamma + \delta = 1$ . This is a linear transformation between two coordinate systems, which we can write in matrix form as

$$\underbrace{\begin{pmatrix} | & | & | & | \\ v_1 & v_2 & v_3 & v_4 \\ | & | & | & | \\ 1 & 1 & 1 & 1 \end{pmatrix}}_{T^{-1}} \underbrace{\begin{pmatrix} \alpha \\ \beta \\ \gamma \\ \delta \end{pmatrix}}_{\lambda} = \underbrace{\begin{pmatrix} x \\ y \\ z \\ 1 \end{pmatrix}}_p \iff T^{-1}\lambda = p \iff \lambda = Tp$$

$T$  always exists because  $v_1, \dots, v_4$  are linearly independent, else it would not be a tetrahedron. By denoting  $T = \{t_{ij}\}_{i,j \in \{1, \dots, 4\}}$ , we can write our barycentric functions as

$$\begin{aligned} \alpha(x, y, z) &= t_{11}x + t_{12}y + t_{13}z + t_{14} \\ \beta(x, y, z) &= t_{21}x + t_{22}y + t_{23}z + t_{24} \\ \gamma(x, y, z) &= t_{31}x + t_{32}y + t_{33}z + t_{34} \\ \delta(x, y, z) &= t_{41}x + t_{42}y + t_{43}z + t_{44} \end{aligned}$$

The convex combination

$$A(x, y, z) = \alpha A_1 + \beta A_2 + \gamma A_3 + \delta A_4$$

is the metric prescribed in the tet. To find  $\nabla \times A$ , let  $A = (A^1, A^2, A^3)$ . We will need the derivatives for the curl, so let

$$(A_j^i)_x \triangleq \frac{\partial A_j^i}{\partial x}$$

be the derivative with respect to  $x$  of entry  $i, j$ . E.g.  $(A_j^i)_x$  is given by

$$(A_j^i)_x = \alpha_x (A_1)_j^i + \beta_x (A_2)_j^i + \gamma_x (A_3)_j^i + \delta_x (A_4)_j^i = t_{11} (A_1)_j^i + t_{21} (A_2)_j^i + t_{31} (A_3)_j^i + t_{41} (A_4)_j^i$$

If we write  $T = (T^1, T^2, T^3, T^4)$  and collect  $(A_k)_j^i$  into a vector

$$\bar{A}_j^i = \begin{pmatrix} (A_1)_j^i \\ (A_2)_j^i \\ (A_3)_j^i \\ (A_4)_j^i \end{pmatrix}$$

this can be shortened to  $\bar{A}_j^{i\top} T^1 = (A_j^i)_x$ . Analogously, we get

$$(A_j^i)_y = \bar{A}_j^{i\top} T^2 \text{ and } (A_j^i)_z = \bar{A}_j^{i\top} T^3$$

The curl is then given by

$$\nabla \times A^i = \begin{pmatrix} (A_3^i)_y - (A_2^i)_z \\ (A_1^i)_z - (A_3^i)_x \\ (A_2^i)_x - (A_1^i)_y \end{pmatrix} = \begin{pmatrix} \bar{A}_3^{i\top} T^2 - \bar{A}_2^{i\top} T^3 \\ \bar{A}_1^{i\top} T^3 - \bar{A}_3^{i\top} T^1 \\ \bar{A}_2^{i\top} T^1 - \bar{A}_1^{i\top} T^2 \end{pmatrix}$$

and  $\nabla \times A = \nabla \times (A^1, A^2, A^3)$ . Notice that the curl is constant within a tetrahedron.

## 4.2 Recursive subdivision

Whenever the rotation coefficient  $R_{pq}$  is needed between some points  $p$  and  $q$ , it is unclear ahead of time how many sampling points on the line  $\ell$  are needed such that  $R_{pq}$  accurately describes how the frame rotates along  $\ell$ . We apply a recursive subdivision scheme to recursively sample more points on  $\ell$  only

where is needed until sampling more points leads to no noticeable improvement anymore (see figure 4.1). We begin by calculating  $R_{ab}$  with just the endpoints. This coefficient is then compared to the result if the midpoint was sampled as well, so i.e. if

$$\frac{||R_{ab} - R_{am} \cdot R_{mb}||_2^2}{\ell^2} < \varepsilon$$

then no measurable improvement happened. We divide by the length of the segment  $\vec{ab}$ , because the segments get smaller and we want the tolerance  $\varepsilon$  to remain the same. This approach has the advantage of only sampling points where there is improvement. See section 7 for results.

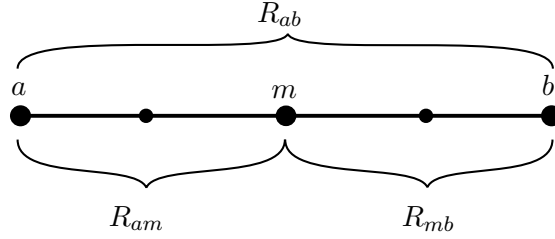


**Figure 4.1.** Points are recursively sampled as midpoints between the line  $\vec{ab}$ . If sampling more points within some line segment leads to noticeable improvement, more points are sampled.

The following code does what is described above.

---

**Algorithm 1** Recursive Subdivision

---

```

1: recursiveDivide ( $a, b$ )
2:    $R_1 = \text{Rotation}(a, b)$ 
3:    $\ell = \text{length}(a - b)$ 
4:    $\text{midpoint} = \frac{a+b}{2}$ 
5:   if  $\frac{||R_1 - \text{Rotation}(a, \text{midpoint}) \cdot \text{Rotation}(\text{midpoint}, b)||_2^2}{\ell^2} < \varepsilon$ 
6:     return  $R_1$ 
7:   else
8:     return  $\text{recursiveDivide}(a, \text{midpoint}) \cdot \text{recursiveDivide}(\text{midpoint}, b)$ 

```

---



## Chapter 5

# Algorithm for $R$ between two arbitrary points in a mesh

To measure the Dirichlet energy, we need to calculate the rotation coefficient  $R$  between two arbitrary points  $q$  and  $p$  that do not necessarily lie within the same tetrahedron. Since the metric and curl is different in each tet, we need to be able to efficiently determine all tets that get intersected by the straight line from  $q$  to  $p$ , and use the correct metric for each corresponding line segment. The calculation for the coefficient then works in the following way:

---

**Algorithm 2** Rotation coefficient  $R$  between  $q$  and  $p$

---

```
1: Input  $(q, p)$ 
2:   //returns all tets intersected by the line  $\vec{pq}$  with the line segments within them
3:    $\text{LINESEGMENTS} \leftarrow \text{tetFinder}(q, p)$ 
4:    $R \leftarrow \text{Id}$ 
5:   for each  $\text{SEGMENT}$  in  $\text{LINESEGMENTS}$ 
6:      $R \leftarrow R \cdot \text{calcCoeff}(\text{SEGMENT})$ 
7: return  $R$ 
```

---

The missing component here is how to efficiently find all tetrahedra that get intersected. One possibility would be to use ray-triangle intersection and test against the whole mesh, but this is not practical, as we have local information that we can exploit.

We use the idea of the straight walk from *Walking in a Triangulation*[3], which relies only on so called *orientation tests* to determine which triangles we traverse.

### 5.1 Framework

Let  $\mathcal{T}$  be a triangulation of a domain  $\Omega$  that is convex. The straight walk traverses all triangles that get intersected by the line segment from  $q$  to  $p$ . The algorithm first makes an initialization step to get into a valid state, then the straight walk can start. To get a feeling how the algorithm works, let us go through an example in 2D. If the algorithm was in a valid state before, the line from  $q$  to  $p$  intersects with some edge  $\vec{lr}$ . Two triangles share this edge. We test on which side point  $p$  lies of this edge to decide whether the walk continues. If the walk continues, we jump through the edge to hop from the old triangle to a new one. This triangle is defined by three vertices  $(l, r, s)$ . We decide if the new candidate point  $s$  lies on the left side or right side of the line from  $q$  to  $p$ . If  $s$  lies on the left, point  $l$  is moved, else point  $r$  is moved. A new edge intersected with the ray  $\vec{qp}$  is found and the walk repeats. This process is illustrated in Figure 5.1

Notice how the ray  $\vec{qp}$  always intersects the edge  $\vec{lr}$  at each update step. We can use this observation to add each edge at each update step to a list. When the algorithm terminates, we can just iterate over this

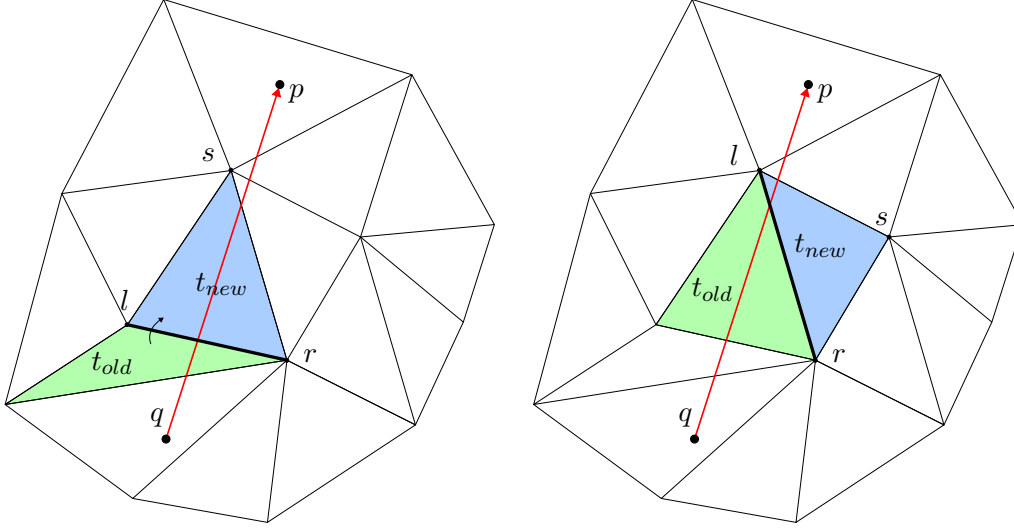


**Figure 5.1.** Straight walk step

list, find the intersection point of the ray  $\vec{qp}$  with the edge and calculate the rotation coefficient for this segment. The straight walk in 3d works similarly. The initialization step consists of finding a starting tet  $t$  where  $q$  is contained. Then, we find the face of the tet  $t$  that gets intersected by the ray  $\vec{qp}$ . Again, at each step, we know that the ray goes out of our current tet  $t$  through some face  $e$  defined by vertices  $uvw$ . We decide if the walk continues by checking on which side  $p$  lies relative to  $e$ . If the walk should continue, we hop through  $e$  to a new tet  $t_{new}$ . With two orientation tests we decide which of the vertices  $u, v, w$  gets moved to the new candidate point  $s$ . This defines a new face  $e_{new}$  where our ray intersects and the walk repeats. Degenerate cases such as when the ray  $\vec{qp}$  goes exactly through a vertex or when the ray lies within a face, the algorithm may get into an invalid state, where the algorithm may then traverse through cells that do not get intersected by the ray. We need to detect and escape those degenerate cases through some additional checks. These are not described in the paper[3]. In most cases, a simple reinitialization is enough when the invalid state is detected.

### 5.1.1 A note on orientation tests

To determine on which side some point  $s$  lies relative to two other points  $q, p$  (that represent a line) in 2D, the geometric *orientation* predicate is used. It corresponds to evaluating the sign of a determinant. Analogously in 3D, the orientation predicate tests whether a fourth point lies above or below a plane defined by three other points. How “above” the plane is defined depends on the ordering within the determinant. In this case, it is above if point  $a$  sees the triangle  $bcd$  when turning counterclockwise (see figure 5.2).

$$\begin{aligned} \text{orientation}(\alpha, \beta, \gamma) &= \text{sign} \left( \begin{vmatrix} \beta_x - \alpha_x & \gamma_x - \alpha_x \\ \beta_y - \alpha_y & \gamma_y - \alpha_y \end{vmatrix} \right) \\ \text{orientation}(\alpha, \beta, \gamma, \delta) &= \text{sign} \left( \begin{vmatrix} \beta_x - \alpha_x & \gamma_x - \alpha_x & \delta_x - \alpha_x \\ \beta_y - \alpha_y & \gamma_y - \alpha_y & \delta_y - \alpha_y \\ \beta_z - \alpha_z & \gamma_z - \alpha_z & \delta_z - \alpha_z \end{vmatrix} \right) \end{aligned}$$

It is important that the sign of the determinant is evaluated exactly. If geometric predicates are implemented with floating point arithmetic, the answers may be inconsistent and wrong. Because of the finite mantissa in floating point representation [1], many numbers cannot be represented exactly. The machine needs to round a number  $x$  to its nearest number that is exactly representable. Many times, roundoff errors occur, a famous example of this is  $0.1 + 0.2 = 0.30000000000000004$ . We call the distance between two exactly representable floating point numbers *machine epsilon*  $\epsilon$ . See figure 5.3 for how this machine epsilon can cause trouble (Example from <http://groups.csail.mit.edu/graphics/classes/6.838/S98/meetings/m12/pred/m12.ht>).



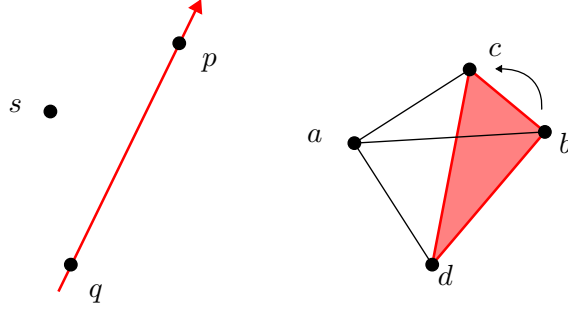


**Figure 5.2.** Orientation predicate: Point  $a$  lies above the plane  $bcd$  because it sees the points in counter-clockwise order,  $orientation(a, b, c, d) > 0$

Logical decision based on floating point arithmetic is correct most of the times, but not always. To fix

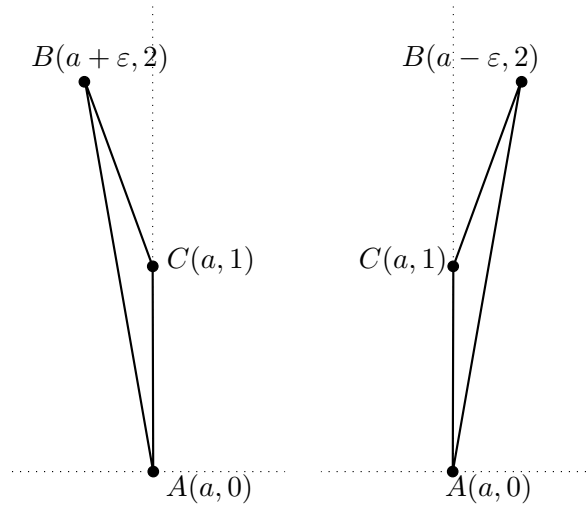


**Figure 5.3.** The orientation predicate implemented with floating point arithmetic cannot distinguish these two cases. The orientation test calculates  $(a + \varepsilon) - a$ . If  $a = 0$ , the orientation test is strictly positive. If  $a = 1$ , then the result is 0, because during the calculation the machine had to round.

this issue, we make use of exact predicates that are implemented with arbitrary precision [14]. Inputs to the orientation test subroutines are assumed to be exact, and we can be sure that the result has the correct sign.

## 5.2 Algorithm *tetFinder*

The final algorithm to find all intersected tetrahedra between two points is as follows.

The algorithm uses several subroutines which are described here:

- `neighbor(t through uvw)` returns the tetrahedron sharing face  $uvw$  with tetrahedron  $t$
- `vertex of t,  $s \neq u, s \neq v, s \neq w$`  returns the remaining vertex of a tetrahedron whose other three vertices are known
- `initialization()`

---

**Algorithm 3** tetFinder

---

```
1: Input  $(q, p)$ 
2:    $t = \text{LocateTet}(q)$ 
3:    $\text{initialization}(t)$ 

4:   //  $qp$  intersects triangle  $uvw$ 
5:   //  $wvqp, vuqp, uwqp$  are positively oriented
6:    $\text{LINESEGMENTS} = []$ 
7:    $\text{PREV} = q$ 
8:    $\text{CURR} = \text{intersection}(qp, uvw)$ 

9:    $\text{LINESEGMENTS.add}([t, \text{PREV}, \text{CURR}])$ 

10:  while  $\text{orientation}(u, w, v, p) > 0$  {
11:     $t = \text{neighbor}(t \text{ through } uvw)$ 
12:     $s = \text{vertex of } t, s \neq u, s \neq v, s \neq w$ 
13:     $\text{PREV} = \text{CURR}$ 
14:    if  $\text{orientation}(u, s, q, p) > 0$  //  $qp$  does not intersect triangle  $usw$ 
15:      if  $\text{orientation}(v, s, q, p) > 0$  //  $qp$  intersects triangle  $vsw$ 
16:         $u = s$ 
17:      else //  $qp$  intersects triangle  $usv$ 
18:         $w = s$ 
19:    else //  $qp$  does not intersect  $usv$ 
20:      if  $\text{orientation}(w, s, q, p) > 0$  //  $qp$  intersects triangle  $usw$ 
21:         $v = s$ 
22:      else //  $qp$  intersects triangle  $vsw$ 
23:         $u = s$ 
24:     $\text{CURR} = \text{intersection}(qp, uvw)$ 
25:     $\text{LINESEGMENTS.add}([t, \text{PREV}, \text{CURR}])$ 
26:  } //  $t$  contains  $p$ 
27:   $\text{LINESEGMENTS.add}([t, \text{PREV}, p])$ 
```

---

## Chapter 6

# Frame Field optimization

- Problem statement
- Simone algorithm from a high level
- Caching of coefficients



## Chapter 7

# Experiments

In this section, the frame field generation applied to a cube mesh with some different metrics is discussed. *Setup:* We store the associated matrices of the metric field at each vertex of the tet mesh. The cube has corners at  $(0, 0, 0)$  and  $(1, 1, 1)$ . The frame field optimization is run to depth 3.

To start, we apply the constant metric  $g^{1/2} = \text{diag}(1, 1, 1)$  everywhere. The rotation coefficients  $R$  are the identity matrix everywhere, as the metric does not twist or squish the space within the field. The result is the boundary aligned frame field with no singularities, as the energy can be minimised to zero if the frames are constant. Figure 7.1 shows the mesh used to store the metric and the resulting constant frame field.

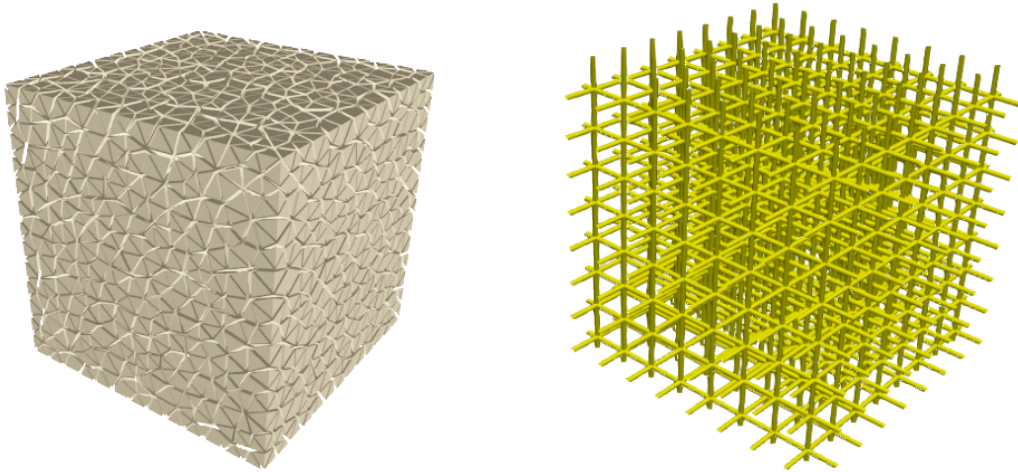


**Figure 7.1.** Left: The mesh used to store the metric field. Right: Constant metric everywhere which gives the boundary aligned constant frame field with no singularities.

To further validate the frame field generation, we divide along the cube along the  $z$ -axis into three equally sized parts. The function to attach the metric to the vertices is then defined as

$$g^{1/2}(z) = \begin{cases} \text{diag}(1, 1, 1) & 0 < z < 1/3 \\ \text{diag}(27z - 8, 1, 27z - 8) & 1/3 < z < 2/3 \\ \text{diag}(10, 1, 10) & 2/3 < z < 1 \end{cases}$$

The metric is constant in the  $y$ -axis and constant-linear-constant in the  $x, z$ -axis. Thus, the rotation coefficients are only of the form

$$\begin{pmatrix} \cos(\alpha) & 0 & \sin(\alpha) \\ 0 & 1 & 0 \\ -\sin(\alpha) & 0 & \cos(\alpha) \end{pmatrix}$$

for some angle  $\alpha$ . The result is depicted in figure 7.2.

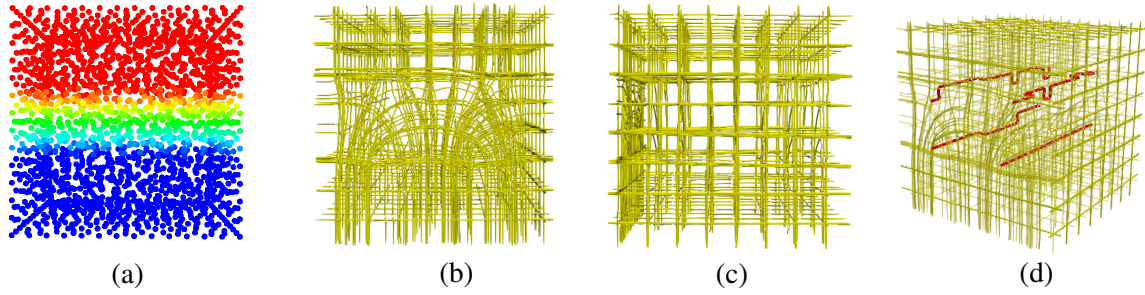


**Figure 7.2.** (a) The varying  $g_{00}^{1/2}$  component along the  $z$ -axis. Visible is how the streamlines of the frame field only change in the middle third (b) and how the frames do not change along the  $y$ -axis (c). The singularities (d) are only points when taking a slice along the  $y$ -axis.

- As a sanity check, we start with the constant metric everywhere.  
constant metric everywhere -  $\zeta$  no singularities
- linearly increasing metric in  $z$ -axis, isotropic scaling
- 2d example anisotropic scaling, constant-linear-constant
- larger cubes at the edges of the cube, isotropic scaling

## **Chapter 8**

# **Conclusion**

The conclusion looks back at the entire work, gives a critical look, summarizes, and discusses extensions and future work.





## **Appendix A**

### **Extra material**

Extra material may be placed in an appendix that appears after the conclusion.



# Bibliography

- [1] *IEEE standard for binary floating-point arithmetic*. New York: Institute of Electrical and Electronics Engineers, 1985. Note: Standard 754–1985.
- [2] D. Bommes, M. Campen, H.-C. Ebke, P. Alliez, and L. Kobbelt, “Integer-grid maps for reliable quad meshing,” *ACM Trans. Graph.*, vol. 32, jul 2013.
- [3] O. Devillers, S. Pion, M. Teillaud, T. Logiciel, and P. Prisme, “Walking in a triangulation,” *International Journal of Foundations of Computer Science*, 03 2001.
- [4] X. Fang, J. Huang, Y. Tong, and H. Bao, “Metric-driven 3d frame field generation,” *IEEE Transactions on Visualization and Computer Graphics*, vol. 29, no. 4, pp. 1964–1976, 2023.
- [5] J. Huang, Y. Tong, H. Wei, and H. Bao, “Boundary aligned smooth 3d cross-frame field,” *ACM Trans. Graph.*, vol. 30, p. 1–8, dec 2011.
- [6] J. M. Lee, *Riemannian Manifolds: An Introduction to Curvature*. 1997.
- [7] J. M. Lee, *Introduction to Smooth Manifolds*. 2000.
- [8] H. Liu, P. Zhang, E. Chien, J. Solomon, and D. Bommes, “Singularity-constrained octahedral fields for hexahedral meshing,” *ACM Trans. Graph.*, vol. 37, jul 2018.
- [9] M. Nieser, U. Reitebuch, and K. Polthier, “Cubecover– parameterization of 3d volumes,” *Computer Graphics Forum*, vol. 30, no. 5, pp. 1397–1406, 2011.
- [10] D. Panozzo, E. Puppo, M. Tarini, and O. Sorkine-Hornung, “Frame fields: Anisotropic and non-orthogonal cross fields,” *ACM Trans. Graph.*, vol. 33, jul 2014.
- [11] C. Papachristou, *Aspects of Integrability of Differential Systems and Fields: A Mathematical Primer for Physicists*. 01 2020.
- [12] N. Pietroni, M. Campen, A. Sheffer, G. Cherchi, D. Bommes, X. Gao, R. Scateni, F. Ledoux, J. Remacle, and M. Livesu, “Hex-mesh generation and processing: A survey,” *ACM Trans. Graph.*, vol. 42, oct 2022.
- [13] N. Ray and D. Sokolov, “On smooth 3d frame field design,” *CoRR*, vol. abs/1507.03351, 2015.
- [14] J. Richard Shewchuk, “Adaptive precision floating-point arithmetic and fast robust geometric predicates,” *Discrete & Computational Geometry*, vol. 18, pp. 305–363, Oct 1997.
- [15] A. Vaxman, M. Campen, O. Diamanti, D. Bommes, K. Hildebrandt, M. B.-C. Technion, and D. Panozzo, “Directional field synthesis, design, and processing,” in *ACM SIGGRAPH 2017 Courses*, SIGGRAPH ’17, (New York, NY, USA), Association for Computing Machinery, 2017.



# Erklärung

*Erklärung gemäss Art. 30 RSL Phil.-nat. 18*

Ich erkläre hiermit, dass ich diese Arbeit selbstständig verfasst und keine anderen als die angegebenen Quellen benutzt habe. Alle Stellen, die wörtlich oder sinngemäss aus Quellen entnommen wurden, habe ich als solche gekennzeichnet. Mir ist bekannt, dass andernfalls der Senat gemäss Artikel 36 Absatz 1 Buchstabe r des Gesetzes vom 5. September 1996 über die Universität zum Entzug des auf Grund dieser Arbeit verliehenen Titels berechtigt ist.

Für die Zwecke der Begutachtung und der Überprüfung der Einhaltung der Selbständigkeitserklärung bzw. der Reglemente betreffend Plagiate erteile ich der Universität Bern das Recht, die dazu erforderlichen Personendaten zu bearbeiten und Nutzungshandlungen vorzunehmen, insbesondere die schriftliche Arbeit zu vervielfältigen und dauerhaft in einer Datenbank zu speichern sowie diese zur Überprüfung von Arbeiten Dritter zu verwenden oder hierzu zur Verfügung zu stellen.

---

Ort/Datum

---

Unterschrift